Journal Name

COMMUNICATION

Rapid microwave assisted synthesis of nearly monodisperse aqueous CuInS$_2$/ZnS nanocrystals

Yatin J. Mange,[a] Melissa R. Dewi,[a] Thomas J. Macdonald,[ab] William M. Skinner[a] and Thomas Nann[ac]*

A rapid microwave-assisted synthesis for nearly monodisperse CuInS$_2$/ZnS nanocrystals (NCs) has been developed. CuInS$_2$/ZnS NCs have been prepared in water using thioglycolic acid as a stabilising ligand. The proposed synthesis results in stable and monodisperse NCs after only 5 minutes. In addition, the NCs were tested as potential sensitisers for photoanodes.

Semiconducting nanocrystals (NCs) may be attractive alternatives to organic dyes in sensitised photoelectrodes[1–8]. They offer size-tunable optical and electronic properties, high absorption coefficients, hot electron extraction and potentially multiple exciton generation[9–11]. Chalcopyrite copper indium disulfide (CuInS$_2$) NCs are of particular interest due to their low toxicity, direct band gap of 1.45eV and absorption/luminescence characteristics ranging from the ultra-violet (UV) to the near infra-red end of the electromagnetic spectrum[12]. In order to improve the luminescence and stability of NCs, zinc is often introduced[13]. The introduction of zinc by cation exchange[14] or shelling[15] are the two most common approaches reported in the literature. Our previous work on CuInS$_2$/ZnS NCs investigated their cation exchange with zinc[14] and more recently, their use in solar cells[16]. There are several routes for the synthesis of CuInS$_2$/ZnS NCs such as thermolysis[17], photochemical deposition[18] and the hot-injection method[19] to achieve monodispersity. However, most of them follow an organic approach such as use of dodecanethiol as solvent, sulfur source and also as surface ligand, which renders their applicability limited due to their hydrophobic nature[20,21]. The elimination of sterically demanding organic solvents such as octadecene (ODE), aids their chemical attachment to metal oxide surfaces such as TiO$_2$[22] and NiO[16]. There are many strategies by which

hydrophobic NCs can be made hydrophilic such as silica shell capping[23], ligand exchange[24,25,26] and amphiphilic polymer coatings[27]. The drawbacks of these methods include the decrease in photoluminescent quantum yield (PLQY) when NCs are transferred to water[28]. Furthermore, the silica shell around the NCs is relatively thick introducing trapping layers, increasing the overall size of the particles and preventing access to the NC surface. All of these approaches are time consuming and controlling the reaction conditions such as temperature and growth time is often not accurate.

Microwave-assisted synthesis of NCs may have several advantages compared with conventional approaches: the method offers short reaction times, rapid and uniform heating characteristics and the resulting NCs exhibit narrow size distribution and high purity[29,30]. In direct comparison with the hot injection method, microwave-assisted methods have distinct advantages including higher penetration of the microwave radiation resulting in homogenous heating of the material which is favorable for uniform nucleation and also formation of monodisperse NCs[31]. Another advantage of microwave-assisted synthesis is the rapid rise in temperature because of the high utilization factor of microwave energy. This results in an increase in the reaction rate by 1 to 2 orders of magnitude[32]. Thus, in sufficiently short time a successive epitaxial process of crystal growth occurs to form NCs, which in turn reduces the concentration of surface defects[31]. Microwave-assisted synthesis can be considered an effective strategy for making high-quality NCs. However, most of the research in this area is focused towards the synthesis of CdTe[31,33–35] and CdSe[30,33,36–39] NCs, a minority focuses on CuInS$_2$[40].

We present a quick and rapid microwave-assisted method for the synthesis of thioglycolic acid coated CuInS$_2$/ZnS NCs *via* an aqueous approach. CuInS$_2$/ZnS NCs were synthesised after 5 minutes yielding nearly monodisperse NCs, which have been characterised, by transmission electron microscopy (TEM) and dynamic light scattering (DLS). These NCs have also been

a. Ian Wark Research Institute, University of South Australia, SA, Australia
b. Department of Chemistry, University College London, London, United Kingdom
c. MacDiarmid Institute for Advanced Materials and Nanotechnology, School of Chemical and Physical Sciences, Victoria University of Wellington, Wellington, New Zealand. E-mail: thomas.nann@vuw.ac.nz

CrystEngComm Accepted Manuscript

tested for their potential use as sensitisers for water splitting or quantum dot sensitized solar cells (QDSSCs)[41].

The procedure to synthesise these NCs builds upon our previous work with some modifications[14] (Materials and methods in ESI): In our synthesis 500 µL Cu(Ac)$_2$ (1.25 mmol) and 500 µL InCl$_3$ (1.25 mmol) were added to a flask containing 37.5 mL of deionised water (degassed) under argon at room temperature. Following this 250 µL of a 1:5 thioglycolic acid to water aqueous solution was added as stabilising agent which caused the reaction mixture turn black and then clear again. The pH of the mixture was then adjusted to approximately 11 by adding 1 M NaOH solution. Once the pH was 11, 250 µL of aqueous Na$_2$S (2.5 mmol) was added causing an immediate deep orange color change. To this, 90 mg of zinc acetate was added and 6 mL of this reaction mixture was transferred into a glass vessel and placed in the microwave reactor (Discover LabMate CEM, USA). The reaction mixture was irradiated with 300 W of microwaves for 5 minutes at 90 ^{0}C. The resulting mixture had a pH of 9 and was luminescent under UV excitation, which confirms the formation of the NCs. The resulting mixture could be used as such or precipitated by adding ethanol followed by centrifugation at 15000 rpm and washing several times with ethanol. Following this, the CuInS$_2$/ZnS powder was dried in a desiccator for 1 – 2 hours. The CuInS$_2$/ZnS powder thus obtained was used for further characterisation.

The photoluminescence (PL) spectra of the CuInS$_2$/ZnS NCs in Fig. 1 show emission around 590 nm. In Fig. 1 the broad emission band extends across the near infrared region. This feature is consistent with the emission spectra of CuInS$_2$/ZnS NCs synthesised by other methods[14,21]. A small shoulder can be observed in the emission spectra in the lower energy region around 700 nm. Such a feature was attributed to the inhomogeneity of NCs[42] and the contribution of defect sites to the overall emission[43]. Given the direct bulk band-gap of 1.55 eV (~800nm) for CuInS$_2$, larger impurities might also contribute. The FWHM of the CuInS$_2$/ZnS NCs was found to be ~108 nm and to our knowledge this is the narrowest FWHM for aqueous CuInS$_2$/ZnS NCs synthesised *via* the microwave method. Our FWHM is also slightly narrower compared with CuInS$_2$/ZnS NCs synthesised *via* conventional method[14]. A small shoulder around 530 nm can be observed in the PL spectra of the core NCs (Fig. S1, ESI). The shoulder disappears upon addition of zinc, which correlates to our previous studies where the copper vacancies are being filled by zinc[14]. The absorption spectra for the core and CuInS$_2$/ZnS NCs can be found in the supporting information (Fig. S2, ESI). They exhibit a broad characteristic shoulder rather than a sharp excitonic peak mainly due to the dominance of internal and surface defects[43]. Fig. S3 of in the ESI shows the tauc plot which was generated from the absorption spectra revealing a band gap of ~2.0 eV. This value was consistent with our previous reports of CuInS$_2$/ZnS NCs and further verified from the photoluminescence spectra.[16] The quantum yield of the synthesised NCs was found to be approximately 1%. Due to the

low quantum yield, it was not possible to obtain an accurate measurement for the lifetime of the NCs. Future work will focus on increasing the QY of the NCs by optimizing the doping of the core-shell structures.
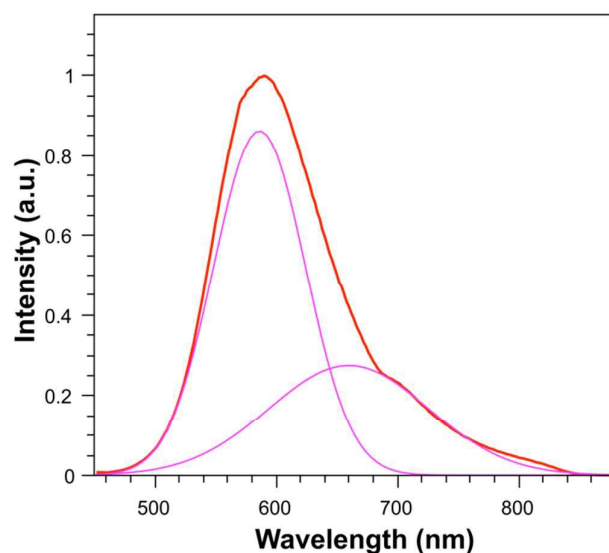

Fig. 1. Emission spectra of aqueous CuInS$_2$/ZnS NCs. The purple line shows the gaussian fit for the emission curve.

Fig 2 (a-b) shows the Transmission Electron Micrographs (TEM) of the CuInS$_2$/ZnS NCs indicating a nearly monodisperse distribution of the particles with an average particle diameter of 5.2 ± 1.32 nm, which was calculated from the TEM images (Fig. S4, ESI). In addition to TEM, the particle diameter was confirmed by DLS measurements, which showed the hydrodynamic diameter of the NCs (Fig. S5, ESI), the slightly larger diameters can be attributed to the TGA stabilising ligands and the solvation shell.

To confirm the CuInS$_2$/ZnS crystal structure, high-resolution (HR) TEM and X-Ray Diffraction (XRD) patterns have been recorded. An inter-fringe distance of 3.2 Å (Fig. 2c) has been observed by HR-TEM. This distance correlates with the (112) crystallographic plane of the NC cores and was also found in the respective XRD (Fig. 2e and Fig. S6, ESI) and selected area electron diffraction (SAED – Fig. 2d) patterns obtained during the TEM analysis. In general, the XRD pattern of the CuInS$_2$ core agrees well with the JCPDS file of roquesite plotted in Fig. 2e. The pattern of CuInS$_2$/ZnS NCs shows additional diffraction peaks, which clearly correspond with the main reflections of ZnS (cf. JCPDF data of zinc blende). Thus, this XRD pattern represents a mixture of roquesite and zinc blende, which is what we expect for the core/shell particles.
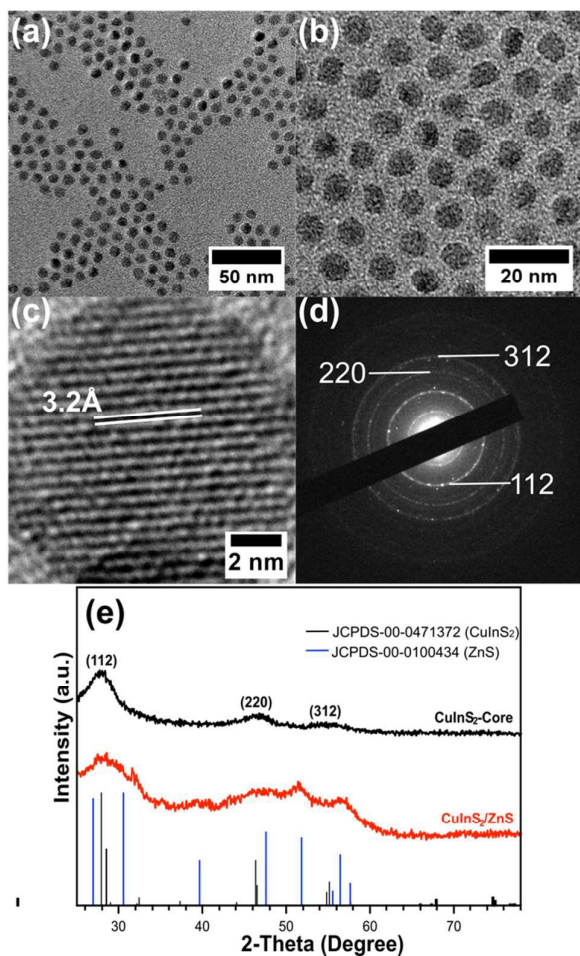
COMMUNICATION

Fig. 2. (a) TEM micrograph of CuInS$_2$/ZnS NCs; (b) HR-TEM of CuInS$_2$/ZnS NCs; (c) HR-TEM showing lattice fringes of CuInS$_2$/ZnS NCs to be 3.2 Å; (d) SAED of CuInS$_2$/ZnS NCs indicating diffraction patterns; (e) XRD patterns of CuInS$_2$-Core and CuInS$_2$/ZnS NCs and the respective JCPDS files for CuInS$_2$ and ZnS.

The elemental composition of CuInS$_2$/ZnS NCs was measured using X-Ray photoelectron spectroscopy (XPS). The S 2p spectrum for the NCs is depicted in Fig. 3. The spectrum consists of a major envelope between ~160 eV and 167 eV binding energy, and a small sulphate contribution near 168 eV. The main envelope requires four (4) S 2p doublets (2p3/2 and 2p1/2 spin orbit components) to be fitted acceptably. Contributions consistent with S-Zn and S in a CuInS$_2$ environment (coordinated to two Cu and two In) are located near 2p3/2 binding energies of 161.3 eV and 162.3 eV, respectively[16]. A strong signal typical of TGA-Cu was observed near 163.4 eV binding energy, and a final contribution appears near 164.6 eV binding energy. The latter environment has been noted for a TGA-Cu precipitate[44] and has been suggested to be a dimer (TGA$_2$) in that work. However it is also possible, given the sulphide substrate and the presence of sulphate, that some polysulphide may also be present. Further evidence of retained TGA ligand was found in the C 1s spectrum (inset),

also consistent with the previous TGA-Cu precipitate work[40], and the elevated carbon surface concentration.
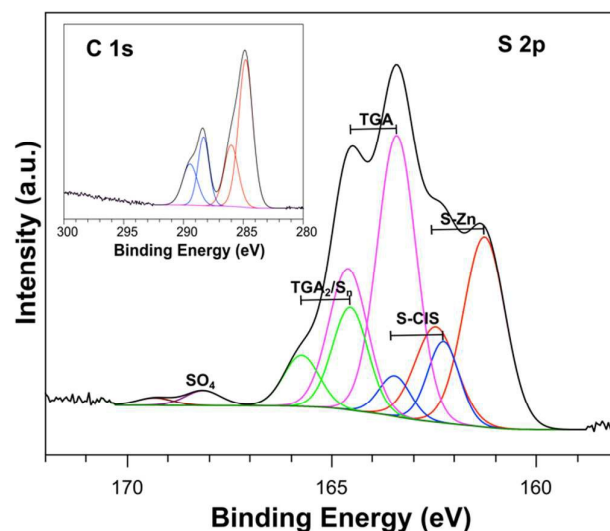

Fig. 3. XPS spectra of S(2p) recorded from CuInS$_2$/ZnS NCs. Inset shows the C(1s) spectra.

The NCs were tested as sensitisers for TiO$_2$ photoanodes. Doctor blade technique was used to coat the TiO$_2$ paste (see ESI for TiO$_2$ paste formation) onto the ITO coated glass slide followed by sintering the electrodes at 450 ^{0}C for 2 hours. CuInS$_2$/ZnS NCs were bound to TiO$_2$ by immersing TiO$_2$ electrodes in the CuInS$_2$/ZnS NC solution for 24 hours resulting in a color change from white to red. Chemical attachment of the NCs onto the TiO$_2$ surface was aided via the thiol and carboxyl moieties. The electrodes were then rinsed with distilled water to remove any unbound NCs.
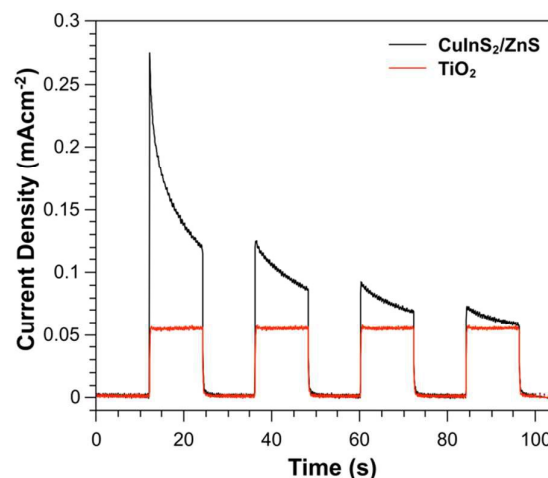

Fig. 4. Photocurrents for TiO$_2$-CuInS$_2$/ZnS NCs (black) and bare TiO$_2$ (red).

Fig. 4 shows the photocurrents of bare TiO_2 and $CuInS_2$/ZnS NCs sensitised TiO_2 as a function of time. $CuInS_2$/ZnS sensitised electrodes exhibited photocurrents that were higher than that of bare TiO_2. The NCs increase the photocurrent initially but degrade rapidly. This has been previously reported and attributed to photo-oxidation of the NCs[14]. Altering the surface ligands and investigating different modes of chemical attachment may increase the stability. Further work on stabilising the NCs for use in energy applications is required.

In conclusion, we have developed a rapid microwave-assisted route for synthesising $CuInS_2$/ZnS NCs in an aqueous medium. The microwave-assisted synthesis of NCs was achieved in 5 minutes, producing nearly monodisperse particles. This work also shows that the NCs may be used in applications for sensitising wide band gap semiconductors such as TiO_2.

Notes and References

1   C.-H. M. Chuang, P. R. Brown, V. Bulović and M. G. Bawendi, *Nat Mater*, 2014, **13**, 796–801.
2   P. V. Kamat, *J. Phys. Chem. Lett.*, 2013, **4**, 908–918.
3   J. Tang, K. W. Kemp, S. Hoogland, K. S. Jeong, H. Liu, L. Levina, M. Furukawa, X. Wang, R. Debnath, D. Cha, K. W. Chou, A. Fischer, A. Amassian, J. B. Asbury and E. H. Sargent, *Nat. Mater.*, 2011, **10**, 765–771.
4   O. E. Semonin, J. M. Luther, S. Choi, H.-Y. Chen, J. Gao, A. J. Nozik and M. C. Beard, *Science*, 2011, **334**, 1530–1533.
5   A. H. Ip, S. M. Thon, S. Hoogland, O. Voznyy, D. Zhitomirsky, R. Debnath, L. Levina, L. R. Rollny, G. H. Carey, A. Fischer, K. W. Kemp, I. J. Kramer, Z. Ning, A. J. Labelle, K. W. Chou, A. Amassian and E. H. Sargent, *Nat. Nanotechnol.*, 2012, **7**, 577–582.
6   T. J. Macdonald and T. Nann, *Nanomaterials*, 2011, **1**, 79.
7   S. Chandrasekaran, T. J. Macdonald, Y. J. Mange, N. H. Voelcker and T. Nann, *J. Mater. Chem. A*, 2014, **2**, 9478–9481.
8   S. Chandrasekaran, T. J. Macdonald, A. R. Gerson, T. Nann and N. H. Voelcker, *ACS Appl. Mater. Interfaces*, 2015, **7**, 17381–17387.
9   W. A. Tisdale, K. J. Williams, B. A. Timp, D. J. Norris, E. S. Aydil and X.-Y. Zhu, *Science*, 2010, **328**, 1543–1547.
10   J. B. Sambur, T. Novet and B. A. Parkinson, *Science*, 2010, **330**, 63–66.
11   C. Smith and D. Binks, *Nanomaterials*, 2013, **4**, 19–45.
12   T. Pons, E. Pic, N. Lequeux, E. Cassette, L. Bezdetnaya, F. Guillemin, F. Marchal and B. Dubertret, *ACS Nano*, 2010, **4**, 2531–2538.
13   J. C. Bear, N. Hollingsworth, A. Roffey, P. D. McNaughter, A. G. Mayes, T. J. Macdonald, T. Nann, W. H. Ng, A. J. Kenyon, G. Hogarth and I. P. Parkin, *Adv. Opt. Mater.*, 2015, **3**, 704–712.
14   T. J. Macdonald, Y. J. Mange, M. Dewi, A. McFadden, W. M. Skinner and T. Nann, *CrystEngComm*, 2014, **16**, 9455–9460.
15   C.-Q. Zhu, P. Wang, X. Wang and Y. Li, *Nanoscale Res. Lett.*, 2008, **3**, 213–220.

16   T. J. Macdonald, Y. J. Mange, M. R. Dewi, H. U. Islam, I. P. Parkin, W. M. Skinner and T. Nann, *J. Mater. Chem. A*, 2015, **3**, 13324–13331.
17   S. L. Castro, S. G. Bailey, R. P. Raffaelle, K. K. Banger and A. F. Hepp, *Chem. Mater.*, 2003, **15**, 3142–3147.
18   J. J. Nairn, P. J. Shapiro, B. Twamley, T. Pounds, R. von Wandruszka, T. R. Fletcher, M. Williams, C. Wang and M. G. Norton, *Nano Lett.*, 2006, **6**, 1218–1223.
19   R. Xie, M. Rutherford and X. Peng, *J. Am. Chem. Soc.*, 2009, **131**, 5691–5697.
20   L. Li, T. J. Daou, I. Texier, T. T. Kim Chi, N. Q. Liem and P. Reiss, *Chem. Mater.*, 2009, **21**, 2422–2429.
21   J. Park and S.-W. Kim, *J. Mater. Chem.*, 2011, **21**, 3745–3750.
22   X. Hu, Q. Zhang, X. Huang, D. Li, Y. Luo and Q. Meng, *J. Mater. Chem.*, 2011, **21**, 15903–15905.
23   Y. Wang, J. Chen and J. Irudayaraj, *ACS Nano*, 2011, **5**, 9718–9725.
24   M. Bruchez, M. Moronne, P. Gin, S. Weiss and A. P. Alivisatos, *Science*, 1998, **281**, 2013–2016.
25   M. R. Dewi, W. M. Skinner and T. Nann, *Aust. J. Chem.*, 2014, **67**, 663–669.
26   M. R. Dewi, G. Laufersky and T. Nann, *RSC Adv.*, 2014, **4**, 34217–34220.
27   T. Pellegrino, L. Manna, S. Kudera, T. Liedl, D. Koktysh, A. L. Rogach, S. Keller, J. Rädler, G. Natile and W. J. Parak, *Nano Lett.*, 2004, **4**, 703–707.
28   S. F. Wuister, I. Swart, F. van Driel, S. G. Hickey and C. de Mello Donegá, *Nano Lett.*, 2003, **3**, 503–507.
29   H.-Q. Wang and T. Nann, *ACS Nano*, 2009, **3**, 3804–3808.
30   J. A. Gerbec, D. Magana, A. Washington and G. F. Strouse, *J. Am. Chem. Soc.*, 2005, **127**, 15791–15800.
31   Y. He, H.-T. Lu, L.-M. Sai, W.-Y. Lai, Q.-L. Fan, L.-H. Wang and W. Huang, *J. Phys. Chem. B*, 2006, **110**, 13352–13356.
32   S. Komarneni, D. Li, B. Newalkar, H. Katsuki and A. S. Bhalla, *Langmuir*, 2002, **18**, 5959–5962.
33   A. L. Washington II and G. F. Strouse, *J. Am. Chem. Soc.*, 2008, **130**, 8916–8922.
34   Y. He, H.-T. Lu, L.-M. Sai, Y.-Y. Su, M. Hu, C.-H. Fan, W. Huang and L.-H. Wang, *Adv. Mater.*, 2008, **20**, 3416–3421.
35   Y. He, L.-M. Sai, H.-T. Lu, M. Hu, W.-Y. Lai, Q.-L. Fan, L.-H. Wang and W. Huang, *Chem. Mater.*, 2007, **19**, 359–365.
36   J. Luo, H. Wei, F. Li, Q. Huang, D. Li, Y. Luo and Q. Meng, *Chem. Commun.*, 2014, **50**, 3464–3466.
37   A. B. Panda, G. Glaspell and M. S. El-Shall, *J. Am. Chem. Soc.*, 2006, **128**, 2790–2791.
38   M. P. Moloney, J. Govan, A. Loudon, M. Mukhina and Y. K. Gun'ko, *Nat. Protoc.*, 2015, **10**, 558–573.
39   Aaron L. Washington and G. F. Strouse, *Chem. Mater.*, 2009, **21**, 2770–2776.
40   W.-W. Xiong, G.-H. Yang, X.-C. Wu and J.-J. Zhu, *ACS Appl. Mater. Interfaces*, 2013, **5**, 8210–8216.
41   M. A. Halim, *Nanomaterials*, 2012, **3**, 22–47.
42   L. De Trizio, M. Prato, A. Genovese, A. Casu, M. Povia, R. Simonutti, M. J. P. Alcocer, C. D'Andrea, F. Tassone and L. Manna, *Chem. Mater.*, 2012, **24**, 2400–2406.
43   D. H. Jara, S. J. Yoon, K. G. Stamplecoskie and P. V. Kamat, *Chem. Mater.*, 2014, **26**, 7221–7228.
44   S. He, D. Fornasiero and W. Skinner, in *Proceedings of the 33rd Australasian Chemical Engineering Conference*, Brisbane, 2005, pp. 548–553.